

INTERACTIONS OF THE CEMENT WITH THE FORMATION IN GEOTHERMAL WELLS

João RMC da Silva and Neil B Milestone*

Callaghan Innovation (formally Industrial Research Ltd), 69 Gracefield Rd, Lower Hutt, New Zealand 5040

neil.milestone@callaghaninnovation.govt.nz

Keywords: *Geothermal cement, hydrothermal cement, well completion, Cement/rock interactions, durability*

ABSTRACT

Cementing the steel casing to the formation is one of the most important operations in completing a well for obtaining steam from geothermal fields. The cement is pumped in to fill the annulus between the steel casing and the formation on the side of the borehole and performs several vital roles. Portland cements are normally used so the binder is a calcium silicate hydrate. The reactions that occur hydrothermally with temperature within the hardened cement are reasonably well known but little is known about the interactions that occur between the cement and the formation. The minerals found in the formation, rhyolite and andesite, when used in conventional concrete can react with cement alkalis to give expansive products which cause cracking and low concrete durability.

Our work has shown that Ca^{2+} and OH^- ions migrate from the cement through to the porous rock forming an interstitial transition zone (ITZ) between cement and rock where new compounds are formed. This migration is modified by additions of silica and interactions with dissolved carbon dioxide. If a layer of drilling mud adheres to the formation, then alternative compounds are formed and a poor cement bond occurs.

1. INTRODUCTION

The cement used for well completion in geothermal fields plays a number of different roles. These include:

- providing a seal between the various layers of the formation
- ensuring high pressure steam reaches the surface and its release can be controlled
- providing support for the steel casing and hopefully, providing corrosion protection to the steel.

The reactions that occur within the cement and additives such as silica are now reasonably well understood, both from the phases formed and their chemical reactions with fluids, particularly those containing CO_2 (Milestone et al. (2012b)). The physical properties required by a cement for geothermal uses were first put forward by the API task Force (1985) and included requirements for compressive strength, chemical stability and permeability together with its bond strength to steel. Surprisingly, no guidelines for bonding to the formation have been reported and little has been published, despite the clear importance of a seal to the formation to prevent loss in steam pressure. Four factors need to be considered, the rock type, the temperature, the geothermal fluid composition and the cement type itself.

The rocks through which geothermal wells are drilled are volcanic. The use in New Zealand of rhyolite and andesite as concrete aggregates has caused problems due to a

reaction known as alkali silica reaction (ASR). In this, the alkalis from Portland cement and silica from the rocks undergo a complex reaction to form an alkali silicate gel which expands, causing cracking in concrete (Freitag et al. 2004). There is some evidence that similar reactions may occur at high temperatures (Poole, 1992; Criaud et al., 1994; Hodgkinson and Hughes, 1999) although the reaction products will be modified. Minerals such as zeolites, katoite, and feldspars can be formed from interaction (Bateman et al., 1998; Hodgkinson and Hughes, 1999) although Andrei and Criaud, (1996) suggested the reaction products remained amorphous.

Temperatures in excess of 300°C can be encountered in geothermal wells which will alter the reaction products, particularly gel hydrates. In New Zealand, the fluids generally contain moderate levels of chloride but in several fields high concentrations of CO_2 in parts of the field render the fluids mildly acidic causing corrosion problems both with casing and cement. (Milestone et al. (1985, 2012a,b)) The presence of CO_2 will also alter the reaction of cement with the formation.

The processes which are responsible for the formation of the microstructure that develops between cement and rock are not well understood. It is clear an interfacial transition zone (ITZ) forms in which the migration of mobile species plays an important part. Reaction of species such as $\text{Ca}(\text{OH})_2$ with the aggregate have been suggested as responsible for a considerable part of the ITZ strength. (Tasong et al. 1998). Very few studies of cement/rock interactions have been carried out at elevated temperatures. Langton et al. (1980) measured shear strengths of cement against a quartzite and a limestone formation at 200°C. They showed that there was movement of both silica and calcium in quartzite but less so in limestone and suggested that the lower strength of the limestone/cement bond was due purely to mechanical bonding rather than a chemical one which occurred with the quartzite.

Work has been conducted on the cement/formation bond and the interactions that occur at low temperatures associated with CO_2 sequestration (Duguid et al., 2006, 2011; Carroll et al., 2009). These studies show that even at these low temperatures, an interaction occurs between the cement and formation which can be affected by the presence of CO_2 . The porosity of the rock was shown to influence the cement/rock bond.

This paper forms part of an extensive work carried out for a PhD thesis (da Silva 2014), describes the interaction that occurs at 150°C between a range of cement formulations that have been used in New Zealand wells and the typical rocks found in our geothermal formations.

2. EXPERIMENTAL

Four different cementing formulations were used to examine rock/cement interactions, both with and without CO_2 injection. These were API Class G cement (G), API Class G + 20 % wt silica flour (G20SF), Class G cement +

40%wt silica flour (G40SF) and Class G cement + 20% Microsilica 600 (G20MS).

XRF analysis of the ignimbrite used is shown in **Table 1** and composition from XRD analysis presented in **Table 2**

	Table 1 - XRF analysis of ignimbrite used											
	SiO_2	Al_2O_3	Fe_2O_3	MnO	MgO	CaO	Na_2O	K_2O	TiO_2	P_2O_5	LOI^a	SUM
IGN	70.56	13.80	2.81	0.04	0.36	1.90	3.75	3.30	0.31	0.07	2.62	99.53

Table 2: Compound composition of ignimbrite

	Feldspars (%)	Quartz (%)	Cristobalite (%)	Tridymite (%)	Kaolinite (%)	Mordenite (%)	Amorphous material (%)	Amorphous silica (%)
IGN	15.0	1.5	N.I.	N.I.	N.I.	N.I.	83.5	59.0

Twenty five mm diameter cavities were cored in small blocks of ignimbrite, which were immersed in geobrine¹ at 90°C for two days to saturate them. Cement slurries were prepared according to API RP10 at a w/s ratio of 0.45 and poured into the different holes. The assemblages were then set/cured for 2 days in geobrine at 90°C before autoclaving for 82 days at 150°C (making a total of 84 days of curing), with a steam pressure of ca. 5 bars. A second set of samples exposed to the same conditions, were cured with a CO_2 overpressure of 6 bars, a typical carbon dioxide concentration in NZ CO_2 enriched fields, making a total pressure of 11 bars. A third set of samples were prepared where a layer of bentonite was applied to the inside of the ignimbrite mould under pressure and then tipped out before the cement slurry was added. These samples were labelled as [cement type]b and were also cured in the autoclave for 82 days (total curing 84 days).

After curing, each cement-rock system was cut in half and samples taken from the ITZ and prepared for X-ray diffraction (XRD), Transmitted Light Optical Microscopy (OM), Scanning Electron Microscopy with Electron Dispersive Spectroscopy (SEM/EDS), Thermogravimetry (TGA) and Mass Spectrometry. Across the ITZ, 4 zones were identified. On the rock side was the parent rock (ROCK) and the ITZ nearest to it (ITZ-R) and the cement side was the cement (CEM) and the ITZ nearest to it (ITZ-C). A small drill was used to remove samples for XRD and TGA from each of the zones.

Polished samples taken across the ITZ were examined by SEM and EDS was used to develop element maps which were combined to produce “phase composition” maps (da Silva, 2014) to allow the migration of ions to be determined. These maps produced zones of different Ca/Si ratios. The cement shows the highest Ca/Si ratio (blue/green colours) as it is Ca rich while the rock shows the lowest Ca/Si ratio (red) as it contains little Ca. The ITZ

shows intermediate Ca/Si compositions depending on the extent of migration of Ca.

3. RESULTS

3.1 G and Gb

XRD showed portlandite ($\text{Ca}(\text{OH})_2$) was found in large amounts in the centre of the cement matrix in these samples, along with $\alpha\text{C}_2\text{SH}$ ² and small quantities of calcite. Portlandite substantially decreases going from G150CEM to G150ITZ-C due to migration of Ca^{2+} (and OH^-) ions across the ITZ into the rock, confirmed by SEM/EDS results. The very distinctive dark ITZ rim (~500 μm) seen by optical microscopy (Fig 1) supports the hypothesis of a reaction rim at the interface where new compounds may form. This rim at 84d is wider than seen at 28d (not shown). New compounds were not seen in G150ITZ-C by XRD, although there was a marked decrease in the amount of portlandite in this zone. The Si concentration across the whole ITZ is relatively uniform and suggests this element moves through the ITZ from the rock, solubilised by OH- ions migrating from the cement into the rock, in a reaction which is not readily detected.

The “phase compositions” of different Ca/Si ratios seen by SEM/EDS (Fig 2) show a significant migration of Ca into the rock. In Fig. 2 the cement is in the top left corner and the Ca/Si ratio decreases to the bottom right corner where the red “phase” signifies the rock. Between these two extremes are the zones of different “phases” with different ca/Si ratios.

The presence of a bentonite layer in Gb changes the reaction sequence. The ITZ is wider and XRD shows the aluminium from bentonite has reacted to form a new crystalline phase, gehlenite (C_2AS), which is a poor binder and where it forms a fissure can develop in the ITZ (Fig 3). Ca penetrates deeper into the rock (up to 600 μm) (Fig 4) and may be driven by cation exchange as aluminium substitution into a silicate network requires a counter cation which Ca can supply.

¹ Recipe for geobrine: 0.19 g sodium sulfate (Na_2SO_4), 0.05 g calcium chloride dehydrate ($\text{CaCl}_2 \cdot 2\text{H}_2\text{O}$), 15.6 g liquid precipitated silica (SiO_2), 4.1 g potassium chloride (KCl), 15.8 g sodium chloride (NaCl) are well mixed and filled with water to make up 20 litres.

² C = CaO ; A = Al_2O_3 ; S = SiO_2 ; H = H_2O

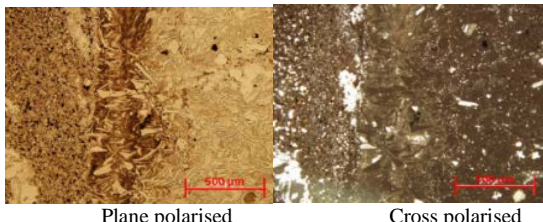


Figure 1: G OM images

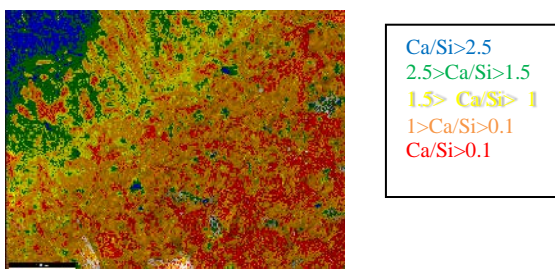


Figure 2: "Phase compositions" of G

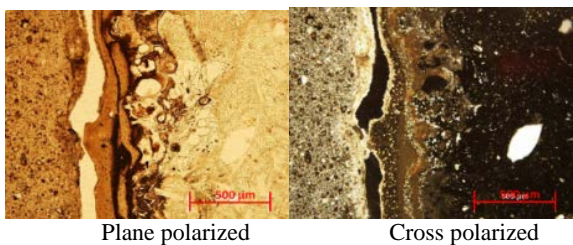


Figure 3: OM image for Gb

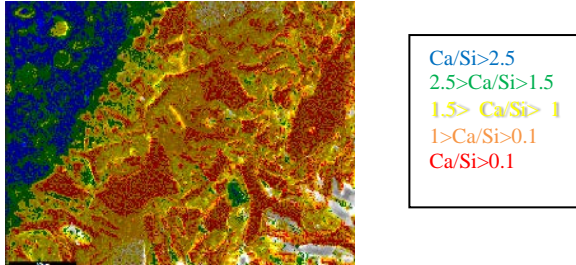


Figure 4: "phase composition" for Gb

3.2 G20SF

A very distinctive ITZ rim is seen by OM (Fig 5) that is wider than in the 28d cured sample (not shown). No portlandite was present in the cement showing it has reacted with the quartz. There is still a distinct ITZ seen with the "phase composition map" (Fig 6). Small amounts of, hillebrandite, C_2SH and killalaite, C_2S_3H along with calcite are concentrated in the ITZ between the cement and rock, indicating that the migrating Ca^{2+} and OH^- ions react with the siliceous glass in the rock to form these compounds.

The light and dark ITZ-R rims that were seen in 28d samples by OM (not shown), have coalesced into a single dark rim that is uniform and slightly wider, indicating that during the second and third months of cure, the Ca^{2+} and OH^- migration driven by concentration gradients still occurs after the cement has hardened. This agrees with SEM/EDS results which show that Ca has penetrated further and in higher amounts into the rock than after 28 days curing.

The addition of bentonite (Fig 7) gives a homogeneous light brown rim seen by OM (PPL). Gehlenite has again formed here as a product of a reaction of Ca migrating from the cement with the Al oxide present in the bentonite, as well as with the SiO_2 present in the bentonite and, perhaps, in the cement (silica flour). Again there is a wider ITZ-R and a weaker cement/rock bond.

The availability of aluminium may have enhanced the formation of tobermorite which is seen in small amounts in the ITZ-C. As explained by Klimesch and Ray (1998), the ready availability of Al makes the formation of tobermorite easier. In the current sample, Al can be supplied into solution from both bentonite and the glass in the ignimbrite as migrating OH^- ions react, along with soluble SiO_2 . Tobermorite will then precipitate in the ITZ.

The seemingly narrower bentonite layer (Fig 7) suggests an increased reaction of the bentonite with silica flour present in the cement but it may depend on the way it has adhered to the rock after being injected in and washed out from the rock cavity. Ca has penetrated deeper supporting evidence for cation exchange from Al substitution driving the migration (Fig 5) but a crack is clearly visible.

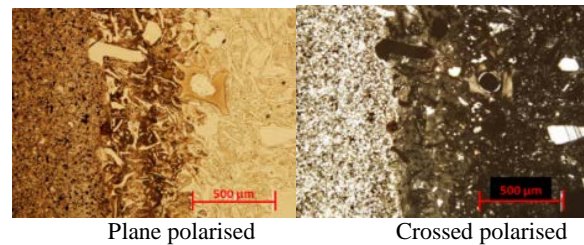


Figure 5: OM image for G20SF

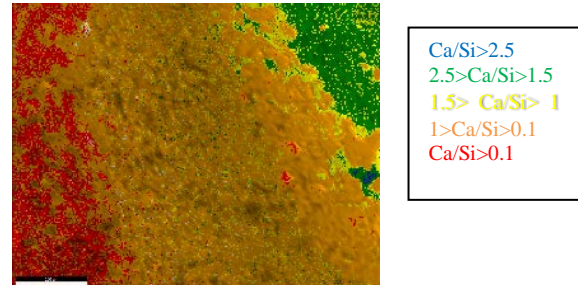


Figure 6: "phase composition" for G20SF

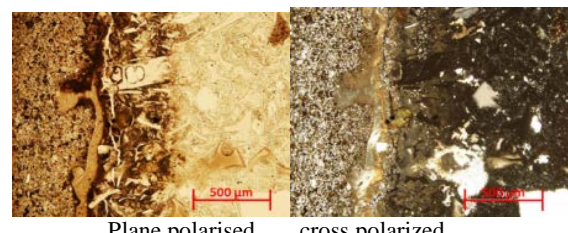


Figure 7: OM image for G20SFb

3.3 G40SF

Tobermorite, $C_5S_6H_5$, is formed in greater amounts in the cement than for the 28d sample (not shown) but large amounts of unreacted quartz remain. Also present is both calcite and aragonite, increasing going from CEM to ITZ-C, showing a higher carbonation rate in the outermost layer. Only traces of calcium silicates and calcium carbonates are

found in the ITZ-R confirming that addition of 40wt% SF slows the migration of cement constituents into the rock. This is supported by the OM results (Fig 9), which shows a considerably narrower ITZ-R than that observed for both G and G20SF.

The “phase composition map (Fig 10) confirms that large additions of silica flour give rise to decreased migration of Ca^{2+} ions across the ITZ although it is wider than the corresponding 28 day sample (not shown) which means that ongoing cement/rock interaction occurs during the second and/or third months of cure.

Again when bentonite is added, gehlenite forms in the ITZ, widening the ITZ-R and weakening the cement/rock bond (Fig 11) and a clear fissure is observed. The ITZ is narrower than for Gb or G20SFb but the higher addition of quartz both dilutes and provides increased reaction sites for Ca making it less likely to migrate. In the “phase composition” map (Fig 12), the limited migration of Ca is much better defined

The increased number of bright spots in the ITZ-C are mostly quartz, which suggests that with the larger amounts of added silica flour, the outermost areas of the cement remain unreacted, as significant amounts of Ca^{2+} and OH^- move into the rock, reducing the amount of these constituents left to react with the quartz from the cement formulation. On the other hand, the small bright grains are probably calcite, which XRD showed was greater in ITZ-C than CEM.

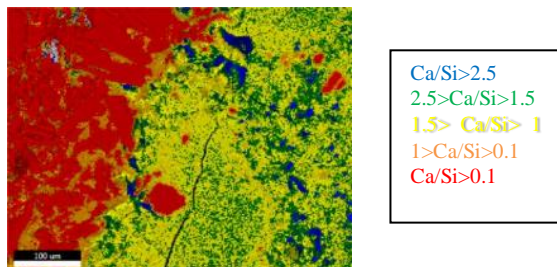


Figure 8: “phase composition for G20SFb

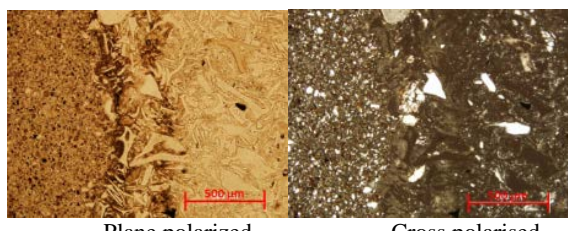


Figure 9: OM image for G40SF

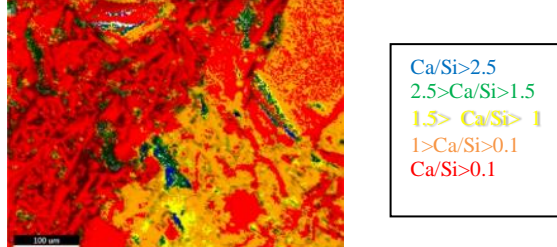


Figure 10: “Phase composition for G40SF

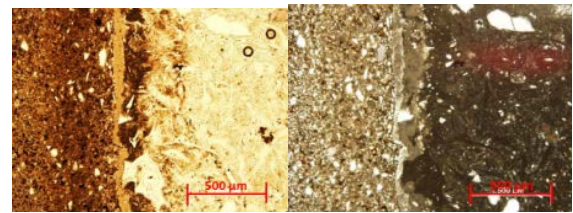


Figure 11: OM image for G40SFb

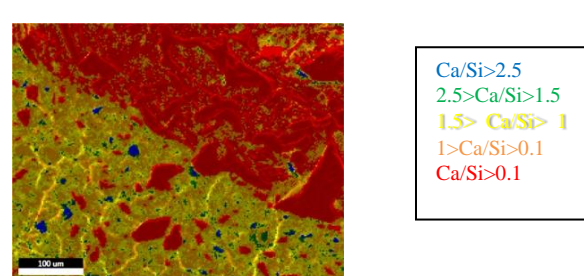


Figure 12: “Phase composition” for G40SFb

3.4 G20MS

Almost no high Ca/Si ratio phases are seen in the phase map across the ITZ (Fig 14), probably due to the fast reaction of the amorphous silica added to the cement which starts reacting at room temperature, unlike quartz which needs a temperature above 120° to react. The ITZ is relatively broad (Fig 13) but does not show the gradual “phase change” as in G. From the element maps, Ca has penetrated over 350μm into the rock, probably through chemical migration.

As in the other samples with bentonite addition, the bentonite barrier is easily distinguishable by OM due to the presence of gehlenite, widening the ITZ-R and weakening the cement/rock bond. (Fig 15). The darker colour of the ITZ-C may be due to the bentonite reacting with the cement and therefore extending the ITZ-C reaction zone so it is the widest of all samples. The clear fissure formed is filled with CaCO_3 .

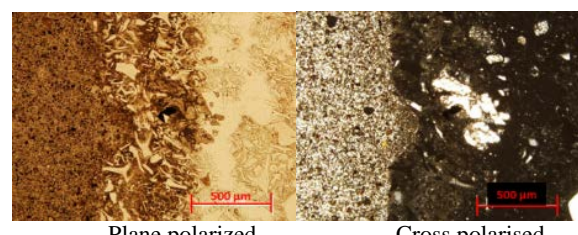


Figure 13: OM image for G20MS (150.84d)

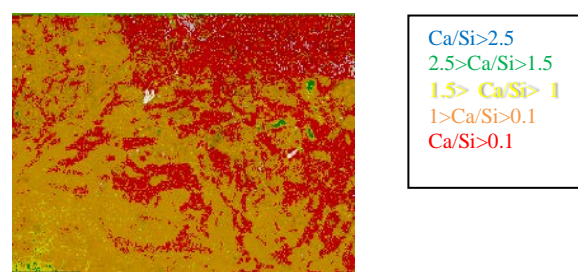


Figure 14: “Phase compositions” for G20MS

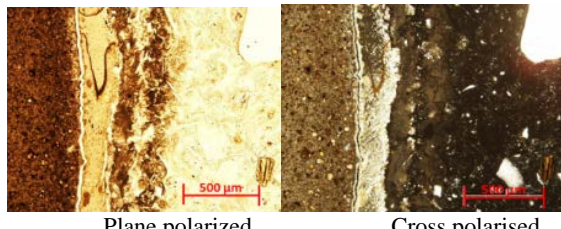


Figure 15: OM image of G20MSb

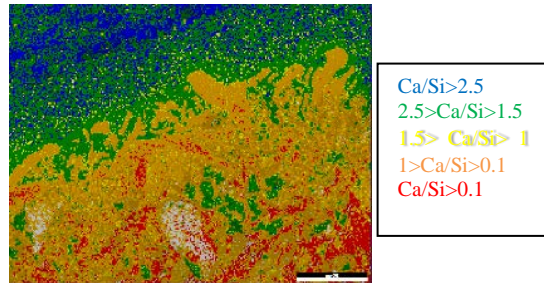


Figure 18: “Phase compositions” for G(CO₂)

4.2 G20SF(CO₂)

In the ITZ, (Fig 19) the amount of aragonite increased from CEM to ITZ-C, meaning there is more carbonation in the outmost layer of the cement due to the increased Ca²⁺ concentration. Traces of tobermorite were found on the edge of the cement nearest ITZ-C. Milestone *et al.* (2012b) showed that the low Ca/Si ratio phase tobermorite could form as Ca²⁺ was removed by CaCO₃ formation during the early curing process lowering the Ca/Si ratio in the cement before the final silicate phases could form. The CaCO₃ formed is largely aragonite but there is significant amorphous carbonate present as seen by thermogravimetry.

The “phase composition” map shows limited Ca²⁺ migration which occurs down the pores of the rock (Fig 20). There is some initial physical movement of fine cement grains into the rock while the cement is fresh.

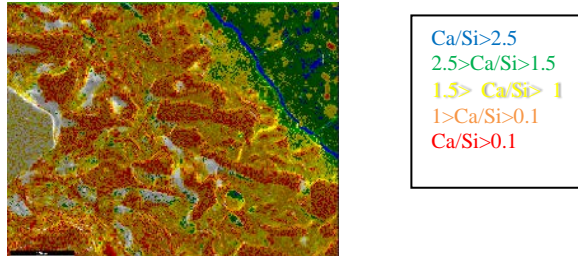


Figure 16: “Phase compositions for G20MSb

4.0 EFFECT OF CARBON DIOXIDE.

The NZ geothermal waters often contain large amounts of CO₂. Samples were exposed to CO₂ while curing at 150°C for 84 days. An ITZ which primarily contained aragonite in the ITZ-CEM, except for the G sample, was clearly visible, up to 2mm wide in some samples.

4.1 G(CO₂)

The ITZ in this sample is around 200μm with a narrow zone of calcite on the edge nearest the cement (Fig 17). Reactions with the rock are limited due to the impermeable sheath of calcite that forms from Ca(OH)₂. Nevertheless, there is still significant Ca²⁺ ion migration (Fig 18) suggesting that for rock interaction migration of OH⁻ ions is also needed as carbonation reduces pH.

The extremely bright ITZ seen by OM indicates the presence of new compound(s), likely to be a product of carbonation. However, XRD of this zone does not indicate large amounts of calcite. Thermogravimetric analysis/mass spectrometry indicates that it is a carbonate but CO₂ loss is at a much lower temperature than expected and points to an amorphous CaCO₃ stabilised by the amorphous silica present. (Kellermeier *et al.*, 2010).

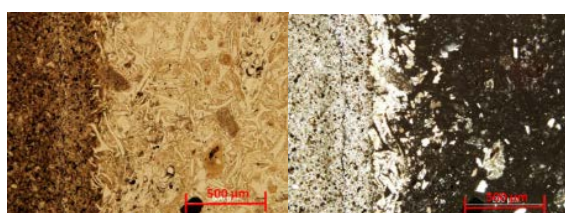


Figure 17: OM images for G(CO₂)

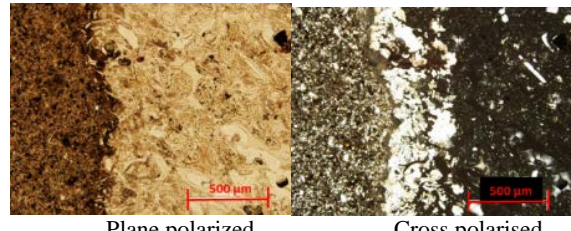


Figure 19: OM image for G20SF(CO₂)

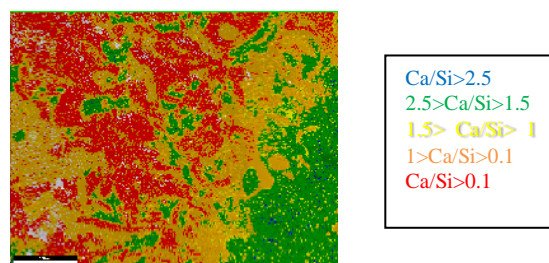


Figure 20: “Phase composition” of G20SF(CO₂)

4.3 G40SF(CO₂)

The carbonation layer is readily visible as a thick, pink, outer-layer formed in the cement and easily distinguishable by OM (Figs 21 and 22). It ranges from ca. 2 to 4 mm thick and depends on the thickness of the surrounding rock. This is in accordance with the work by Duguid *et al.* (2011), who observed a decrease in the cement degradation rate with the increase of the surrounding rock thickness.

The amount of Ca²⁺ ion migration into the rock is limited as seen in Fig. 23 and confined to the rock pores.

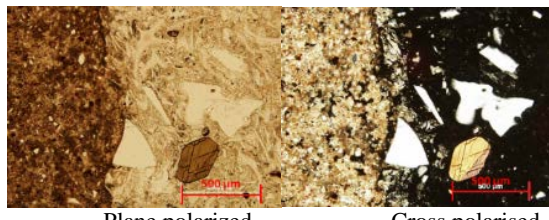


Figure 21: OM image for G40SF(CO₂)

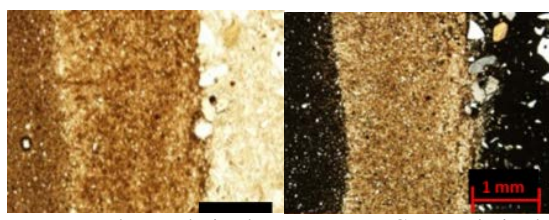


Figure 22: Detail of carbonation zone on cement side of ITZ in G40SF(CO₂)

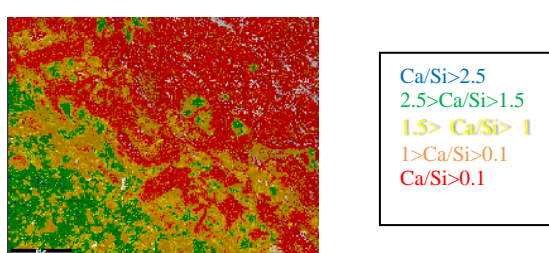


Figure 23: "Phase composition" in G40SF(CO₂)

4.4 G20MS(CO₂)

The ITZ-R and the Ca migration into the rock is similar to that observed for G20SF although the carbonation layer is less (Fig 24). There is a marked reduction in CaCO₃ formed as the fine silica reacts rapidly.). The Ca²⁺ ion migration is less than for G20SF(CO₂) due to the rapid reaction of Ca(OH)₂ with both SiO₂ and CO₂ (Fig 25) and again confined to the rock pores.

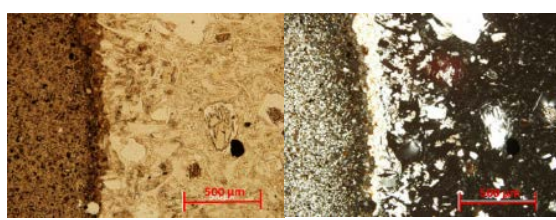


Figure 24: OM image for G20SF(CO₂)

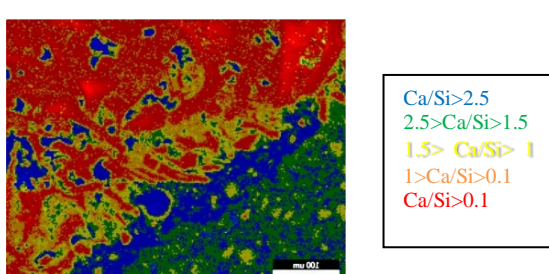


Figure 25: "Phase composition" in G20MS(CO₂)

5.0 CONCLUDING REMARKS

Interaction of a Portland based well cement with the rock formation in geothermal wells forms a clear reaction rim or interstitial transition zone (ITZ) surrounding the cement which has a different composition and chemistry than either the cement or the rock. Ca²⁺ and OH⁻ ions migrate across this zone and interact with the rock. The movement of Ca occurs in two ways. Initially there is physical movement of fine cement particles into the porous formation before the cement hardens, which is followed by a slow chemical migration of Ca²⁺ and OH⁻ ions which react with the glass in the formation rocks. The initial physical movement is dictated by cement particle size and formation porosity but in a porous formation, can lead to increased bonding between the rock and cement.

The slower chemical migration of Ca²⁺ and OH⁻ ions through the ITZ depends on several factors: the cement formulation and silica content, the surrounding fluid composition as well as the rock type and the presence or absence of drilling mud. Increasing amounts of silica reduce movement of Ca²⁺ ions as Ca²⁺ ions are 'fixed' within the hardened cement, with a reactive silica (MS600) proving very effective in limiting Ca²⁺ movement. Substitution of aluminium from bentonite into a silicate structure requires a counter cation and Ca can migrate to fill this role. Ca migration continues after the cement has hardened and the binding calcium silicate hydrates have formed.

The presence of a layer of bentonite such as that from drilling mud, causes decreased bonding between the cement and formation. The bentonite reacts with the cement (and possibly silica from the amorphous glass released by OH⁻ ions giving rise to a crystalline aluminosilicate, gehlinitite, which is a weak binder. In an extreme case, its formation can cause separation of the cement and rock, leading to a fissure up which fluid can escape. In carbonated water this fissure may fill with CaCO₃.

Carbon dioxide readily penetrates the porous rock matrix and competes with silica for Ca²⁺ ions forming CaCO₃ and decreasing the Ca/Si ratio of the binder matrix. When present, this carbonate layer forms part of the ITZ and can lead to tobermorite formation. The extent of carbonation depends on the Ca/Si ratio of the cement formulation. The initial Ca carbonate formed is largely amorphous, stabilised by dissolved silica and will slowly crystallise with time. Metastable aragonite forms from carbonation of calcium silicate hydrates while calcite will only form if Ca(OH)₂ is present.

ACKNOWLEDGEMENTS

This work has been funded by MBIE through Programme C08X0902, Cements for Extreme Environments, with co-funding from an industrial consortium of Mighty River Power, Contact Energy, Halliburton and Baker Hughes.

REFERENCES

Andrei V. and A. Criaud, (1996), Alkali-aggregate reactions products identified in concrete after high temperature cure in alkaline solution", 10th Int. Conf. on AAR, Melbourne, Australia, p. 957-964

API Task Force, (1985), API work group reports field tests of geothermal cements, *Oil Gas J.* Feb 11 93-97

Bateman K., P. Cooms, D.J. Noy, J.M. Pearce and P.D. Wetton, (1998), Numerical modelling and column experiments to simulate the alkaline disturbed zone around a cementitious waste repository, *Proc. Mat. Res. Soc. Symp.* 506,605-611

Carroll, S.A., W.W. McNab and S.C. Torres, (2011), Experimental study of cement-sandstone/shale-brine-CO₂ interactions, *Geochem. Trans.* 12(9) 1-19

Criaud A., C. Defossé, B. Chabanis, L. Debray; B. Michel, D. Sorrentino, M. Gallias, M. Salomon, S. Guédon and A. Le Roux, (1994), The French standard methods for evaluating the reactivity of aggregates with respect to AAR: results of an inter-laboratory program, *Cem. Concr. Comp.*, 16(3), 199-206.

Da Silva, J.R.M., (2014) Cement/rock interaction in geothermal wells, PhD thesis presented at Victoria University of Wellington, New Zealand

Duguid, A.; Radonjic, M; Scherer, G.W. (2006); The effect of carbonated brine on the interface between well cement and geologic formations under diffusion-controlled conditions, *8th International Conference on Greenhouse Gas Control Technologies*, Trondheim, Norway

Duguid, A., M. Radonjic and G.W. Scherer, (2011), Degradation of cement at the reservoir/cement interface from exposure to carbonated brine, *Int. J. Greenhouse Gas Control*, 5, 1413-1428

Freitag, S.A., R. Goguel and N.B. Milestone, (2004) Alkali silica reaction; Minimising the risk of damage to concrete: Guidance notes and recommended practice, TR3; pub. Cement and Concrete Association of New Zealand

Hodgkinson, E.S. and C.R. Hughes, (1999), The mineralogy and geochemistry of cement/rock interactions: high resolution studies of experimental and analogue materials, *Chemical containment of waste in the geosphere*, Geol. Soc. London SP157, 195-211

Kellermeier, M., E. Melero-García, F. Glaab, R. Klein, M. Drechsler, R. Rachel, J. M. García-Ruiz and W. Kunz (2010); Stabilization of amorphous calcium carbonate in inorganic silica-rich environments, *J. Am. Chem. Soc.*, 132, 17859-17866

Klimesch, D.S., and A Ray, (1998), Metakaolinite additions in autoclaved cement/quartz pastes: a ²⁹Si and ²⁷Al MAS NMR investigation, *Adv. Cem. Res.* 10 93-99

Langton C.A., M.W. Gruzeck and D.M. Roy, (1980), Chemical and physical properties of the interfacial region between unreactive aggregate and hydrothermally cured cement, *Cem. Concr. Res.* 10 449-454

Milestone, N.B., T. Sugama, L.E. Kukacka, and N. Carciello, (1985), Effect of CO₂ Attack on Geothermal Cement Grouts, *Geothermal Res. Counc. Trans.* 10, 75-79

Milestone, N.B., C.H. Bigley, A.T. Durant, and M.D.W. Sharp, (2012a), Effects of CO₂ on Geothermal Cements, *GRC Transactions*, 36, 301-306

Milestone, N.B., C.H. Bigley, A.T. Durant, M.D.W. Sharp and J.R.M.C. da Silva, (2012b), Chemical reactions in geothermal cements, *New Zealand Geothermal Workshop 2012 Proceedings* 19-21 November 2012, Auckland, New Zealand

Poole, A.B., (1992), Alkali silica reactivity mechanisms of gel formation and expansion, *Proc. 9th Int. Conf. on AAR, London, UK*, 782-789

Tasong, W.A., J.C. Cripps and C.J. Lynsdale (1998), Aggregate-cement chemical interactions, *Cem. Concr. Res.* 27(8) 1037-1048